Influence of Fat on Differential Receptor Interacting Serine/Threonine Protein Kinase 1 Activity Leading to Apoptotic Cell Death in Murine Liver Ischemia Reperfusion Injury Through Caspase 8

Vasantha L. Kolachala,[1*] Sirish K. Palle,[1*] Ming Shen,[1] Asha Shenoi,[1] Dmitry M. Shayakhmetov,[1] and Nitika A. Gupta[1,2]

Current understanding is that receptor interacting serine/threonine protein kinase 1 (RIPK1) can lead to two distinct forms of cell death: RIPK3-mediated necroptosis or caspase 8 (Casp8)-mediated apoptosis. Here, we report that RIPK1 signaling is indispensable for protection from hepatocellular injury in a steatotic liver undergoing ischemia reperfusion injury (IRI) but not in the lean liver. In lean liver IRI, RIPK1-mediated cell death is operational, leading to protection in RIP1 kinase-dead knock-in ($RIPK1^{K45A}$) mice and necrostatin-1s (Nec1s)-treated lean wild-type (WT) mice. However, when fed a high-fat diet (HFD), $RIPK1^{K45A}$-treated and Nec1s-treated WT mice undergoing IRI demonstrate exacerbated hepatocellular injury along with decreased RIPK1 ubiquitylation. Furthermore, we demonstrate that HFD-fed $RIPK3^{-/-}/Casp8^{-/-}$ mice show protection from IRI, but HFD-fed $RIPK3^{-/-}/Casp8^{-/+}$ mice do not. We also show that blockade of RIPK1 leads to increased Casp8 activity and decreases mitochondrial viability. *Conclusion:* Although more studies are required, we provide important proof of concept for RIPK1 inhibition leading to distinctive outcomes in lean and steatotic liver undergoing IRI. Considering the rising incidence of nonalcoholic fatty liver disease (NAFLD) in the general population, it will be imperative to address this critical difference when treating patients with RIPK1 inhibitors. This study also presents a new target for drug therapy to prevent hepatocellular injury in NAFLD. (*Hepatology Communications* 2019;3:925-942).

Obesity is reaching epidemic proportions worldwide. Moreover, with a spectrum of clinical manifestations ranging from benign steatosis to steatohepatitis, it is estimated that about 10%-25% of patients with nonalcoholic fatty liver disease (NAFLD) may progress to cirrhosis, and it is predicted that NAFLD will become the leading indication for liver transplant by 2020.[1,2] Additionally, NAFLD can also lead to hepatocellular carcinoma (HCC), and it is known that the incidence of HCC of nonviral etiology is also on the rise.[3] It is currently believed that continuous death of liver parenchymal cells resulting in extensive hepatocyte turnover is the fundamental mechanism underlying the progression of benign

Abbreviations: ALT, alanine aminotransferase; BID, BH3-interacting domain death agonist; Casp, caspase; cDNA, complementary DNA; cFLIPs, cellular FLICE-like inhibitory proteins; cIAPs, cellular inhibitor of apoptosis proteins; Co-IP, co-immunoprecipitation; DAPI, 4′,6-diamidino-2-phenylindole; DMSO, dimethyl sulfoxide; FFA, free fatty acid; H&E, hematoxylin and eosin; HCC, hepatocellular carcinoma; HFD, high-fat diet; HIRI, hypoxia ischemia reperfusion injury; Ig, immunoglobulin; IRI, ischemia reperfusion injury; MCDD, methionine-choline-deficient diet; mRNA, messenger RNA; NAFLD, nonalcoholic fatty liver disease; NASH, nonalcoholic steatohepatitis; Nec1s, necrostatin-1s; NF-κB, nuclear factor kappa beta; PI, propidium iodide; RIPK1, receptor interacting serine/threonine protein kinase 1; $RIPK1^{K45A}$, receptor interacting serine/threonine protein kinase 1 kinase-dead knock-in; SDS-PAGE, sodium dodecyl sulfate–polyacrylamide gel electrophoresis; TNFR1, tumor necrosis factor receptor 1; TNF-α, tumor necrosis factor α; TUNEL, terminal deoxynucleotidyl transferase–mediated deoxyuridine triphosphate nick-end labeling; WT, wild type.

Received January 2, 2019; accepted March 11, 2019.

Additional Supporting Information may be found at onlinelibrary.wiley.com/doi/10.1002/hep4.1352/suppinfo.

Supported by the National Institutes of Health (K08 grant DK091506 to N.G.) and the North American Society for Pediatric Gastroenterology, Hepatology, and Nutrition Foundation to N.G. and NIH grant number AI065429 to D.M.S.

**These authors contributed equally to this work.*

hepatic steatosis to steatohepatitis[4] similar to the development of HCC.[5] With the high incidence of obesity and NAFLD, the increased sensitivity of steatotic hepatocytes to injury and death, even in a liver exhibiting only benign steatosis, represents a major clinical problem and is most vividly demonstrated in clinical settings associated with reduced liver perfusion, known as ischemia reperfusion injury (IRI). IRI may result from hepatobiliary surgery, heart failure, shock, and transplantation, and it has been shown that a fatty liver exhibits significantly more adverse clinical outcomes.[6,7] While most studies have explored IRI in lean livers,[8,9] we and others have shown that severe hepatocellular death results from steatotic liver IRI.[10-14] To date, the molecular mechanisms that mediate cell death in a steatotic liver remain poorly defined.

Over recent years, there has been a major advance in our understanding of the complexity of cell signaling pathways that sense, regulate, and execute cell death. Arguably, the most prominent advancement in the field has been the recognition that necrosis can be a highly regulated physiologic process and that necrotic-type cell death can be executed by specialized molecular machinery, including receptor interacting serine/threonine protein kinase (RIPK)1- and RIPK3-dependent necroptosomes,[15-18] caspase (Casp) 1- and Casp11-dependent inflammasomes,[19,20] and Casp8- and Casp9-dependent apoptotic pathways, which have been implicated in mediating hepatocyte cell death in response to a variety of stimuli.[21-23] The canonical bimodal view of cell death types, classified as ordered and regulated (apoptosis) and disordered and catastrophic (necrosis), has been challenged by the abundant evidence that necrosis can also be a physiologically regulated type of cell death.[18,24,25] The function of RIPK1/RIPK3 signaling machinery has been defined as pronecrotic based on the initial findings that RIP1 and RIP3 kinases drive necrosis-like cell death in various cell types in response to tumor necrosis factor receptor 1 (TNFR1) signaling.[25,26] Although the prodeath function of RIPK1/RIPK3 signaling has been confirmed in a large number of subsequent studies in various physiologic and pathophysiologic contexts, a study by Takahashi et al.[27] demonstrated that RIPK1 signaling can also serve a prosurvival function and is essential for maintenance of the intestinal epithelial integrity in the gut.[28] Therefore, although RIP1 kinase is emerging as a multifunctional nexus regulating cellular prosurvival and prodeath decisions,[29] the exact molecular basis that guides the RIPK1 functional commitment in different cell types remains unclear. In this study, we investigated the role of the RIPK1 pathway and the response of lean and steatotic liver when exposed to IRI in a mouse model of fatty liver and in a steatotic hepatocyte cell culture system.

Materials and Methods

REAGENTS AND CELLS

The mouse hepatocyte AML12 cell line (hereafter referred to as hepatocytes unless otherwise specified)

View this article online at wileyonlinelibrary.com.
DOI 10.1002/hep4.1352

Potential conflict of interest: Nothing to report.

ARTICLE INFORMATION:

From the [1]Department of Pediatrics, Emory University School of Medicine, Atlanta, GA; [2]Transplant Services, Children's Healthcare of Atlanta, Atlanta, GA.

ADDRESS CORRESPONDENCE AND REPRINT REQUESTS TO:

Nitika Arora Gupta, M.D., D.C.H., D.N.B.
Associate Professor of Pediatrics
1760 Haygood Drive
Atlanta, GA 30322
E-mail: nitika.gupta@emory.edu
Tel.: +1-404-727-2026

was purchased from ATCC (Manassas, VA). The following were purchased from Sigma-Aldrich (St. Louis, MO): necrostatin-1s (Nec1s; 2263), palmitic acid (P0500), oleic acid (01008), essential fatty acid free bovine serum albumin (A6003), propidium iodide (PI; 81845), tumor necrosis factor α (TNF-α; 6674), and Oil Red O stain (00625). Other materials consisted of MG-1322 (474791; CalBiochem), Casp8 assay kit (K113; Biovision, CA), Pierce co-immunoprecipitation (Co-IP) kit (26149; Thermo Fisher Scientific), high-fat diet (HFD; D12492, 60% fat) and methionine-choline-deficient diet (MCDD) (A06071302) (both from Research Diets, Inc., NJ), Click-iT-Plus terminal deoxynucleotidyl transferase–mediated deoxyuridine triphosphate nick-end labeling (TUNEL) assay kit (C10617; Invitrogen), 3-(4,5-dimethylthiazol-2-yl)-2,5-diphenyltetrazolium bromide (MTT) cell viability assay kit (KA1606; Abnova), ubiquitin antibody (3936; Cell Signaling, Denvers, MA), cleaved Casp8 antibody (9694; Cell Signaling, Denvers, MA), RIPK1 antibody (72139; Abcam), RNA isolation kit (74104; Qiagen), high-capacity complementary DNA (cDNA) reverse transcriptase kit (4368814; Applied Biosystems), and SYBR Select Master mix (4472908; Applied Biosystems). Casp8 mouse-specific primers sequence was as follows: forward, TTCGAGCAACAGAACCACAC; reverse, TTCTTCACCGTAGCCATTCC.

ANIMALS

Four-week-old, male, C57/BL6, wild-type (WT) and TNFR1$^{-/-}$ mice on a C57BL/6 background and J substrain were purchased from the Jackson Laboratory (Bar Harbor, ME) and housed at the Emory University animal facility. All animals received humane care in accordance with protocols approved by the Institutional Animal Care and Use Committee. Mice were maintained on a 12-hour dark–light cycle and allowed free access to food and water under conditions of controlled temperature (25°C ± 2°C). WT mice were placed into three groups: group one fed on regular chow, group 2 on an HFD (12 weeks), and group 3 on an MCDD (6 weeks). From each group, mice were divided into two subgroups: IRI+vehicle (dimethyl sulfoxide [DMSO]/saline) and IRI+Nec1s (in DMSO/saline) (n = 6/group, repeated twice).

RIP1 kinase-dead knock-in (RIPK1^{K45A}), RIPK3$^{-/-}$/Casp8$^{-/+}$, RIPK3$^{-/-}$/Casp8$^{-/-}$, and BH3-interacting domain death agonist (BID)$^{-/-}$ mice on a C57BL/6 background and substrain J were obtained from Dr. Shayakhmetov and Dr. Mocarski (Emory University).[30-32] RIPK3$^{-/-}$/Casp8$^{-/+}$ and RIPK3$^{-/-}$/Casp8$^{-/-}$ were littermates that were weaned after genotyping. These mice were generated because Casp8$^{-/-}$ mice are embryologically lethal. Mice were divided into two groups: group one was fed a regular mouse chow and group two was fed an HFD *ad libitum* for 12 weeks before IRI. Body weights were monitored at regular intervals. Hepatic steatosis was confirmed by Oil Red O staining.

RIPK1 BLOCKADE BY CHEMICAL INHIBITOR Nec1s

To assess the role of RIPK1 in steatotic IRI, we used the RIPK1-specific inhibitor Nec1s. Nec1s has been identified as a highly potent inhibitor of RIP1 kinase-dependent cell death as it blocks the catalytic activity of RIP1 phosphokinase.[33] We gave 12.5 mg/kg of Nec1s[34] in two doses 15 minutes before and 15 minutes after IRI. The Nec1s was dissolved in 30% DMSO (shown to be nontoxic by Thackaberry et al.[35]), diluted in warm saline, and injected intravenously. Control mice received an equal volume of DMSO in saline.

HEPATIC IRI

Animals were anesthetized with pentobarbital (50 mg/kg) and subjected to IRI, as described.[10] Briefly, a clamp was placed on the portal vein and hepatic artery, blocking blood flow to the left and medial lobes of the liver. Partial hepatic ischemia was induced, and the clamp was removed after 40 minutes to allow reperfusion. The mice were killed after 2, 6, and 24 hours of reperfusion, and liver tissue and blood samples were collected.

HISTOLOGIC EVALUATION

Paraffin sections of entire liver lobes from lean and HFD control mice and mice undergoing IRI were stained with hematoxylin and eosin (H&E). Sections were scanned using the brightfield scanner Hamamatsu Nanozoomer 2.0 HT in the Department of Pathology, Emory University. Necrosis scoring (area of necrosis, number of nuclei) was assessed using ImageScope, which is image analysis software from Aperio.[12]

HEPATOCELLULAR INJURY

Hepatocellular injury was assessed *in vivo* in the Division of Animal Resources, Emory University, by measuring serum levels of alanine aminotransferase (ALT).

IN VITRO HYPOXIA ISCHEMIA REPERFUSION INJURY

Mouse hepatocyte cell line AML12 cells were made steatotic by the addition of a mixture of free fatty acids (FFA) consisting of palmitic and oleic acid (400 nm each), as described.[11] The cells were subjected to hypoxia IRI (HIRI) as follows: hypoxia was induced by using a hypoxia chamber (1% O_2, 4% CO_2, 95% N_2), ischemia was induced by removing serum from the media, and reperfusion was induced by adding serum containing medium and placing the cells in the regular incubator at normal atmospheric conditions (20% O_2, 5% CO_2) for different time periods. Lean and steatotic hepatocytes were exposed to HIRI, PI was added to the media, and uptake of PI (red fluorescence) by dead cells was imaged and quantified in real time by the IncuCyte Zoom system (Essen BioScience) for 24 hours.

Casp8 ACTIVITY ASSAY

FFA-treated AML12 cells were treated with and without Nec1s (30 μm)[36] and subjected to HIRI. Total cell lysates were processed for the Casp8 activity assay as per the manufacturer's instructions (BioVision, CA).

TUNEL STAINING

The Click-iT Plus TUNEL assay was used for *in situ* apoptosis detection with Alexa Fluor 488 dye according to manufacturer's instructions (Cat# C10617; Invitrogen).

IMMUNOPRECIPITATION

FFA-treated AML12 cells were subjected to HIRI of 40 minutes ischemia followed by 30 minutes, 1 hour, and 2 hours of reperfusion. MG-132 (10 μm) was added to the media to prevent deubiquitylation.[37] One milligram of total protein from the cell lysate from lean, steatotic with HIRI, and steatotic without HIRI cells was immunoprecipitated by RIPK1-specific antibody (5 μg/mL lysate) and control immunoglobulin (Ig)G lysate using the Pierce Co-IP kit (Thermo Fisher Scientific) as per the manufacturer's instructions. The Co-IP technique was achieved by replacing protein A/G agarose beads with AminoLink Plus resin to which pure immunoprecipitated antibodies can be directly and permanently conjugated. The pulldowns were separated on sodium dodecyl sulfate–polyacrylamide gel electrophoresis (SDS-PAGE) under denatured condition and probed with ubiquitin antibody. These blots were reprobed with RIPK1 antibody to confirm the specificity of the immunoprecipitated protein.

RNA EXTRACTION AND QUANTITATIVE REAL-TIME POLYMERASE CHAIN REACTION

Total RNA was extracted from lean and FFA-treated AML12 cells that were subjected to HIRI and from liver tissues of mice undergoing IRI, using the Qiagen RNeasy kit according to the manufacturer's instructions. RNA was quantified using Nanodrop 2000 spectrophotometry (Thermo Fisher Scientific), and cDNA synthesis was performed with the high-capacity cDNA reverse transcriptase kit using 2 μg total RNA. Real-time quantitative polymerase chain reaction was performed using Bio-Rad Universal SYBR Green Supermix. Relative gene expression was calculated by the comparative ΔΔCt method. Expression levels of the target genes were normalized to the housekeeping gene 18S ribosomal RNA in each sample, and fold change in the target gene expression among experimental groups was compared to controls.

WESTERN BLOT ANALYSIS

Whole liver proteins were extracted from mice liver tissues and AML12 cells after the various treatments described above. Proteins from total cell lysates and proteins subjected to immunoprecipitation with RIPK1 antibody were run on SDS-PAGE and transferred and probed with ubiquitin, RIPK1, and Casp8 antibodies.

IMMUNOFLUORESCENCE

Liver sections from lean and HFD-fed WT mice subjected to IRI, lean, and FFA-treated AML12 cells

undergoing HIRI and human nonalcoholic steatohepatitis (NASH) liver biopsy tissues were subjected to immunofluorescence. The NASH liver biopsy paraffin sections were obtained from the Pathology Department of Children's Healthcare of Atlanta after institutional review board approval. All six liver biopsy sections had 60%-90% steatosis and presence of inflammation. Normal (lean) human liver biopsy sections were obtained from three different donors from Zyagen (HP-314; San Diego, CA). These samples were processed for immunofluorescence by cleaved Casp8 (Ap391) (18C8) rabbit monoclonal primary antibody (#9496; Cell Signaling), which detects cleaved fragments of 43/41 kDa and 18 kDa of Casp8 and secondary antibody conjugated to Alexa Fluor 488 (green) and nuclear stain (blue, 4′,6-diamidino-2-phenylindole [DAPI]). Staining intensities were quantified using Fiji image analysis software.

STATISTICAL ANALYSIS

Groups were compared using the Student *t* test for two groups and analysis of variance for three or more groups, using Prism 6 (GraphPad). Data are represented as mean ± SD; $P < 0.05$ was considered significant. Each experiment was repeated three times.

Results

HFD-FED TNFR1$^{-/-}$ MICE ARE PROTECTED AGAINST HEPATOCELLULAR INJURY FROM IRI

In order to understand which cell death pathways are operational in steatotic livers undergoing IRI, we investigated death receptor TNFR1 and its downstream signaling molecules. Our earlier studies demonstrated increased cell death in WT HFD mice undergoing IRI. TNFR1$^{-/-}$ mice were fed an HFD and showed similar weight gain as the WT mice fed an HFD (Fig. 1A). Interestingly, there was significantly less injury in HFD-fed TNFR1$^{-/-}$ mice compared to HFD-fed WT mice, as outlined by white lines in H&E images ($P < 0.02$; Fig. 1B,C), more intact nuclei ($P < 0.0001$; Fig. 1D), and significantly lower serum ALT ($P < 0.0002$; Fig. 1E). These data demonstrate the critical role that the TNFR1 pathway plays in steatotic hepatocellular injury. To further assess the molecular aspects of cell death mediated through TNFR1, we then examined the role of downstream RIPK1 and RIPK3 as well as Casp8.

BLOCKADE OF RIPK1 BY Nec1s AMELIORATES HEPATOCELLULAR INJURY IN LEAN MICE AND EXACERBATES INJURY IN HFD- AND MCDD-FED MICE UNDERGOING IRI

To investigate the role of RIPK1 in IRI-induced hepatocellular injury, we treated lean mice, HFD-fed mice, and MCDD-fed mice with Nec1s. Compared to vehicle-treated mice, lean mice treated with Nec1s and exposed to IRI exhibited significantly less hepatocellular injury (as determined by the areas outlined in white on H&E images) with a substantially decreased injury area ($P < 0.002$; Fig. 2A,D), increased number of intact nuclei ($P < 0.02$; Fig. 2E), and a significantly lower serum ALT ($P < 0.002$; Fig. 2F). Surprisingly, when the HFD-fed mice were treated with Nec1s and exposed to IRI, we observed completely opposing results. There was exacerbated hepatocellular injury with a significantly increased injury area ($P < 0.02$; Fig. 2B,D), decreased number of intact nuclei compared to saline-treated HFD mice ($P < 0.0001$; Fig. 2E), and substantially higher serum ALT levels ($P < 0.01$; Fig. 2F). In the MCDD mice, treatment with Nec1s also exacerbated liver cell injury induced by IRI. There was a significant increase in area of injury ($P < 0.001$; Fig. 2C,D), substantially fewer intact nuclei compared to vehicle-treated MCDD-fed mice ($P < 0.009$; Fig. 2E), and significantly higher serum ALT ($P < 0.02$; Fig. 2F). Thus, both HFD-fed and MCDD-fed mice demonstrated increased cell death compared to their lean counterparts when administered RIPK1-specific inhibitor Nec1s. These data confirm that Nec1s treatment in a steatotic liver either induced by an HFD or by an MCDD leads to exacerbated hepatocellular injury when exposed to IRI whereas Nec1s treatment is protective in the lean liver. The results of these studies clearly indicate that RIPK1 inhibition leads to opposing functions in the lean (protection from IRI) and steatotic (exacerbated cell death) environment.

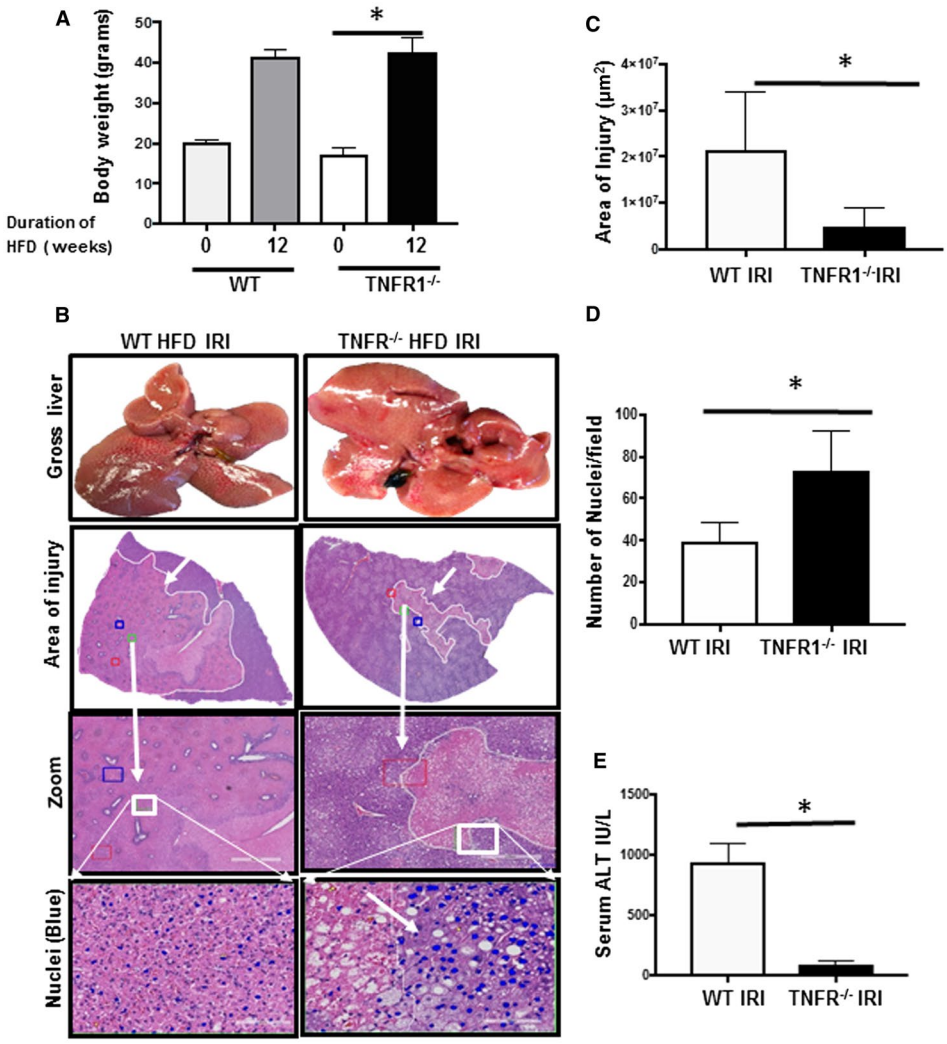

FIG. 1. HFD-fed TNFR1$^{-/-}$ mice are protected against hepatocellular injury from IRI. (A) WT HFD mice and TNFR1$^{-/-}$ HFD mice gained similar body weights 12 weeks after feeding, as shown in the bar graph. (B) Representative liver tissues were obtained from WT HFD IRI mice (left panel) and TNFR1$^{-/-}$ HFD IRI mice (right panel): gross images (first row), H&E stained liver lobe showing the areas of injury marked by white lines (second row), zoomed images of the area of injury (third row, 4×), and intact nuclei (blue, fourth row, 40×). (C) TNFR1$^{-/-}$ HFD IRI mice demonstrated significant reduction in area of injury compared to WT HFD IRI mice (*P < 0.02). (D) The graph shows a significant increase in the number of intact nuclei (*P < 0.0001). (E) The graph shows a significant reduction in serum ALT (*P < 0.0002; n = 12). Data in (A,C-E) represent mean ± SD. * represents Significance.

BLOCKADE OF RIP1 KINASE FUNCTION IN RIPK1^{K45A} MICE AMELIORATES HEPATOCELLULAR INJURY IN LEAN MICE BUT EXACERBATES INJURY IN HFD-FED MICE UNDERGOING IRI

Because RIPK1 blockade by chemical inhibition in two different *in vivo* models of steatotic liver and lean liver showed opposing outcomes (protection in lean and exacerbated hepatocellular injury in steatosis) following exposure to IRI, we wanted to confirm these findings in a RIPK1^{K45A} mouse model because RIPK1$^{-/-}$ mice are embryonically lethal. When fed an HFD, RIPK1^{K45A} (details given in Materials and Methods and Supporting Table S1) mice showed similar weight gain compared to WT mice fed an HFD (Fig. 3A). Lean RIPK1^{K45A} mice showed protection from IRI, whereas HFD-fed RIPK1^{K45A} mice showed

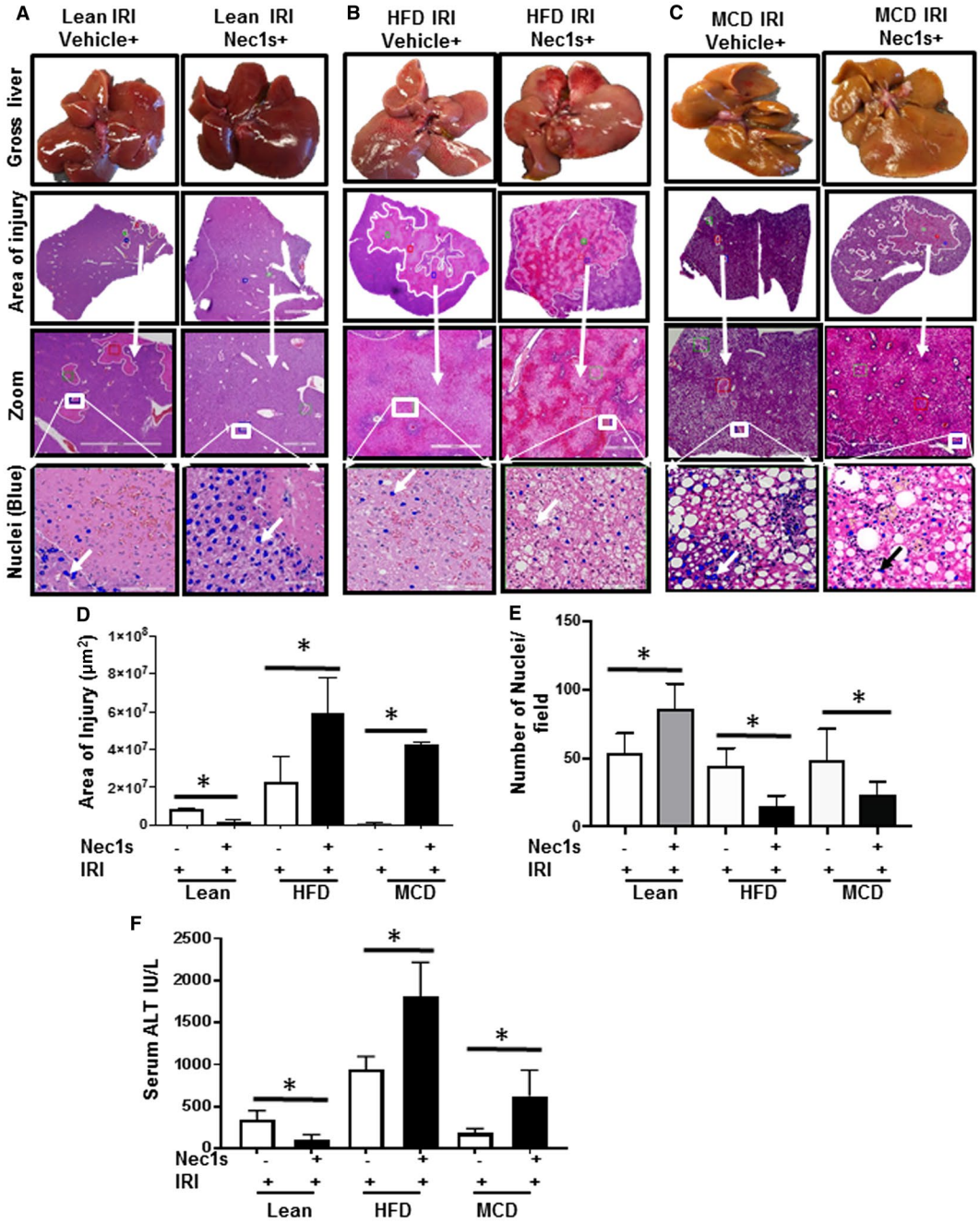

FIG. 2. Blockade of RIPK1 by Nec1s ameliorates hepatocellular injury in lean mice and exacerbates injury in HFD- and MCDD-fed mice undergoing IRI. WT lean, HFD-, and MCDD-fed mice were subjected to IRI along with vehicle or Nec1s (12 mg/kg) intravenous administration, as described in Material and Methods. Rectangles represent the area that was zoomed in the panel below. (A) Representative liver tissues were obtained from lean IRI veh+ (left panels) and lean IRI Nec1s+ (right panels). (B) HFD IRI veh+ (left panels), HDF IRI Nec1s+ (right panels). (C) MCDD IRI veh+ (left panels), MCDD IRI Nec1s+ (right panels). Gross images (first row), H&E stained liver lobe showing the areas of injury marked by white lines (second row), zoomed images of the area of injury (third row), and intact nuclei (blue, fourth row). (D) Lean Nec1s+ demonstrated a significant reduction in area of injury compared to lean veh+ (*$P < 0.002$), whereas, both HFD Nec1s+ and MCDD Nec1s+ showed significant increase in area of injury compared to HFD veh+ (*$P < 0.01$) and MCDD veh+ (*$P < 0.02$). (E) Lean Nec1s+ demonstrated a significant increase in intact nuclei compared to lean veh+ (*$P < 0.02$). Both HFD Nec1s+ and MCDD Nec1s+ showed significantly less intact nuclei compared to HFD veh+ ($P < 0.0001$) and MCDD veh+ ($P < 0.009$). (F) Lean Nec1s+ demonstrated significantly lower serum ALT compared to lean veh+ ($P < 0.002$). In addition, HFD Nec1s+ and MCDD Nec1s+ mice showed significant increase in ALT levels compared to HFD veh+ ($P < 0.02$) and MCDD veh+ ($P < 0.001$; n = 10). Data represent mean ± SD.

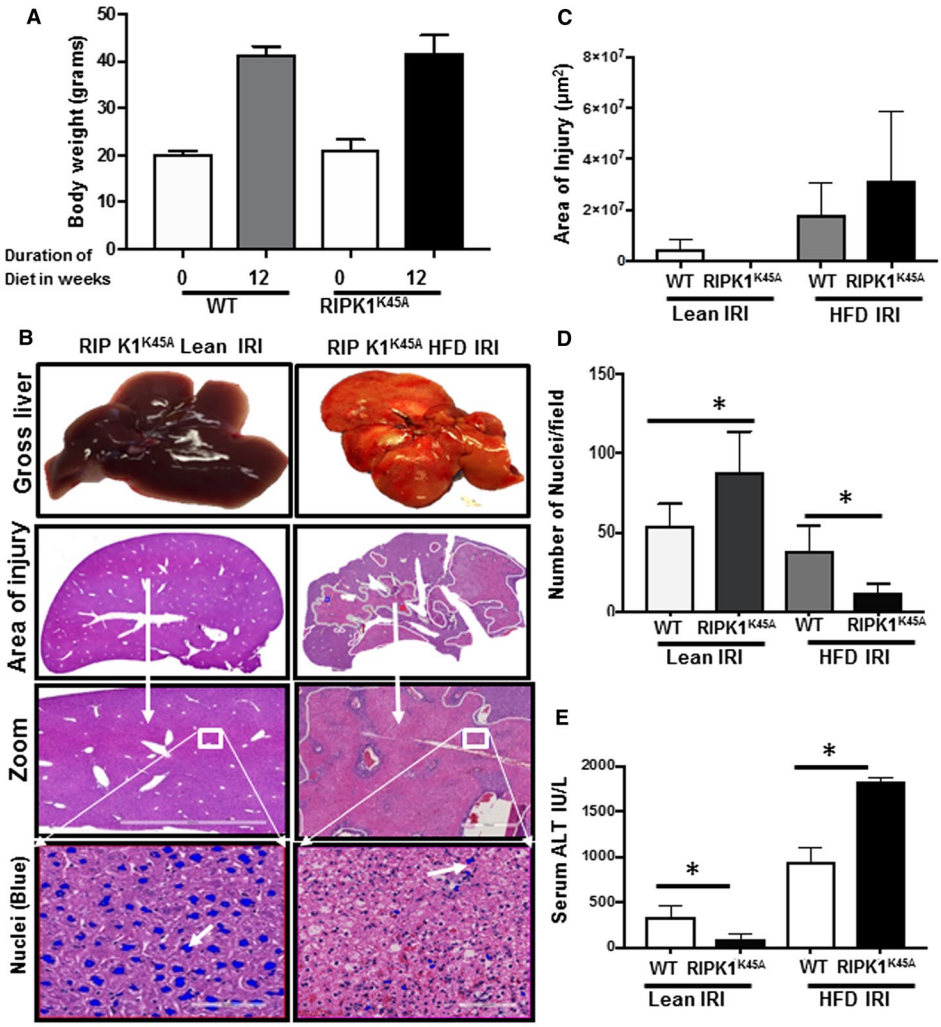

FIG. 3. Blockade of RIP1 kinase function in RIPK1^{K45A} mice ameliorates hepatocellular injury in lean mice but exacerbates injury in HFD-fed RIPK1^{K45A} mice undergoing IRI. Arrow represents zoomed area from the figure above. Rectangle represents the area that was zoomed in the panel below. (A) WT and RIPK1^{K45A} mice fed an HFD gained similar body weights 12 weeks after feeding. (B) Representative images of lean RIPK1^{K45A} IRI (left panel) and HFD RIPK1^{K45A} IRI (right panel). Gross images (first row), H&E stained liver lobe showing the areas of injury marked by white lines (second row), zoomed images of the area of injury (third row, 4×), and intact nuclei (blue, fourth row, 40×). (C) RIPK1^{K45A} lean IRI showed reduced injury area compared to RIPK1^{K45A} HFD IRI. (D) RIPK1^{K45A} lean IRI showed significantly higher number of intact (blue) nuclei compared to RIPK1^{K45A} HFD IRI (*P < 0.0001). (E) RIPK1^{K45A} lean IRI showed significantly lower serum ALT levels compared to RIPK1^{K45A} HFD IRI (*P < 0.0002; n = 10). Data represent mean ± SD.

an increased area of injury from IRI (Fig. 3B,C), fewer intact nuclei (P < 0.0001; Fig. 3B,D), and significantly higher serum ALT (P < 0.000.1; Fig. 3B,E). These data convincingly establish that RIPK1 blockade by chemical or genetic modification leads to opposing effects. Our data show protection from hepatocellular injury in lean liver in contrast to exacerbated injury in steatotic liver. This raises important questions about the applicability and possible detrimental effects of RIPK1 inhibition in humans with fatty liver disease.

BLOCKADE OF RIPK1 BY Nec1s DEMONSTRATED INCREASED CELL DEATH IN FFA-TREATED AML12 CELLS UNDERGOING HIRI

To corroborate the opposing outcomes of RIPK1 inhibition in lean versus steatotic mouse liver (HFD- and MCDD-fed mice), we treated steatotic AML12 cells with Nec1s and exposed them to HIRI, as detailed in Materials and Methods. The number of PI-positive cells (indicating dead cells) were decreased

in Nec1s-treated lean cells compared to vehicle-treated cells undergoing HIRI. However, there was a significant increase in PI uptake in FFA-treated AML12 cells that was further exacerbated with Nec1s treatment, corroborating the *in vivo* findings (Fig. 4A). Further, live imaging of PI uptake (assessing cell death) by lean and FFA-treated AML12 cells by the IncuCyte Zoom system and Nec1s treatment demonstrated similar results; the number of PI-positive cells increased with time in Nec1s-treated steatotic AML12 cells with HIRI (Fig. 4C, green line) compared to steatotic cells without Nec1s treatment (red line). However, in Nec1s-treated lean cells with HIRI, there were fewer PI-positive cells (purple line) compared to vehicle-treated cells (blue line). Graph B shows lean control cells without HIRI, and there was no significant difference between the groups.

UBIQUITYLATED RIPK1 WAS DECREASED IN FFA-TREATED AML12 CELLS AS SHOWN BY IMMUNOPRECIPITATION

Because blockade of RIPK1 in lean and steatotic mice/hepatocytes had opposing effects, we wanted to investigate whether RIPK1 ubiquitylation changes in response to steatosis and HIRI *in vitro*. Ubiquitylation is a critical process involved in the regulation of cell signaling and plays a key role in determining the fate of the cell in response to TNFR1 stimulation.[38] Therefore, we assessed RIPK1 ubiquitylation using immunoprecipitation of RIPK1, as described in the Materials and Methods section. We found ubiquitylation of RIPK1 to be decreased in steatotic hepatocytes undergoing HIRI (Fig. 4D, lane 6) compared to lean hepatocytes (Fig. 4D, lane 5), which showed a significant increase in ubiquitylated RIPK1 (shown in red box), making this a critical difference between the lean and steatotic hepatocytes exposed to HIRI (Fig. 4D, lane 6). To assess the specificity of immunoprecipitation, control IgG was used as a negative control (lanes 7 and 8) and TNF-α-treated cell lysates were used as a positive control (lanes 9 and 10). Specificity of ubiquitylated RIPK1 was confirmed by reprobing the same blot with RIPK1-specific antibody (Fig. 4D, bottom panel). This confirmed that RIPK1 ubiquitylation is seen in lean liver but decreased in the steatotic liver when exposed to IRI, leading to cell survival in lean liver and cell death in steatotic liver.

STEATOTIC LIVER IRI IS NOT MEDIATED THROUGH RIPK3 SIGNALING BUT THROUGH Casp8 SIGNALING

To further define the role of downstream RIPK3 and Casp8 signaling pathways in lean and steatotic liver exposed to IRI, $RIPK3^{-/-}/Casp8^{-/+}$ and $RIPK3^{-/-}/Casp8^{-/-}$ mice were fed an HFD for 12 weeks and subjected to IRI. Details of the mice are given in the Materials and Methods section. These mice showed similar weight gain as WT mice fed an HFD (Fig. 5A). When exposed to IRI, $RIP3^{-/-}/Casp8^{-/+}$ mice exhibited significantly exacerbated injury (as outlined by white lines in H&E images), a phenotype similar to WT mice, suggesting no involvement of RIPK3 in steatotic liver IRI (Fig. 5B, left panel). However, when HFD-fed $RIP3^{-/-}/Casp8^{-/-}$ mice were exposed to IRI, there was hepatocellular protection with a significant reduction in area of injury ($P < 0.001$; Fig. 5B,C), more intact nuclei ($P < 0.0001$; Fig. 5D), and lower serum ALT ($P < 0.002$; Fig. 5E). These findings indicate that $RIP3^{-/-}/Casp8^{-/+}$ did not show protection but instead showed exacerbated hepatocellular injury similar to RIPK1 inhibition. The absence of Casp8 resulted in protection. This alludes to the fact that the exacerbated injury in steatotic liver may be mediated by a Casp8-dependent cell death mechanism.

RIPK1 BLOCKADE LEADS TO INCREASED Casp8 ACTIVITY IN HFD-FED MICE LIVER AND FFA-TREATED AML12 CELLS. HUMAN NASH LIVER BIOPSIES SHOW INCREASED EXPRESSION OF CLEAVED Casp8

To assess the role of Casp8 in steatotic hepatocellular injury, FFA-treated AML12 cells were subjected to HIRI, as described in Materials and Methods. Casp8 messenger RNA (mRNA) levels were significantly higher at 30 minutes after HIRI ($P < 0.01$; Fig. 6A). Additionally, when these cells were subjected to

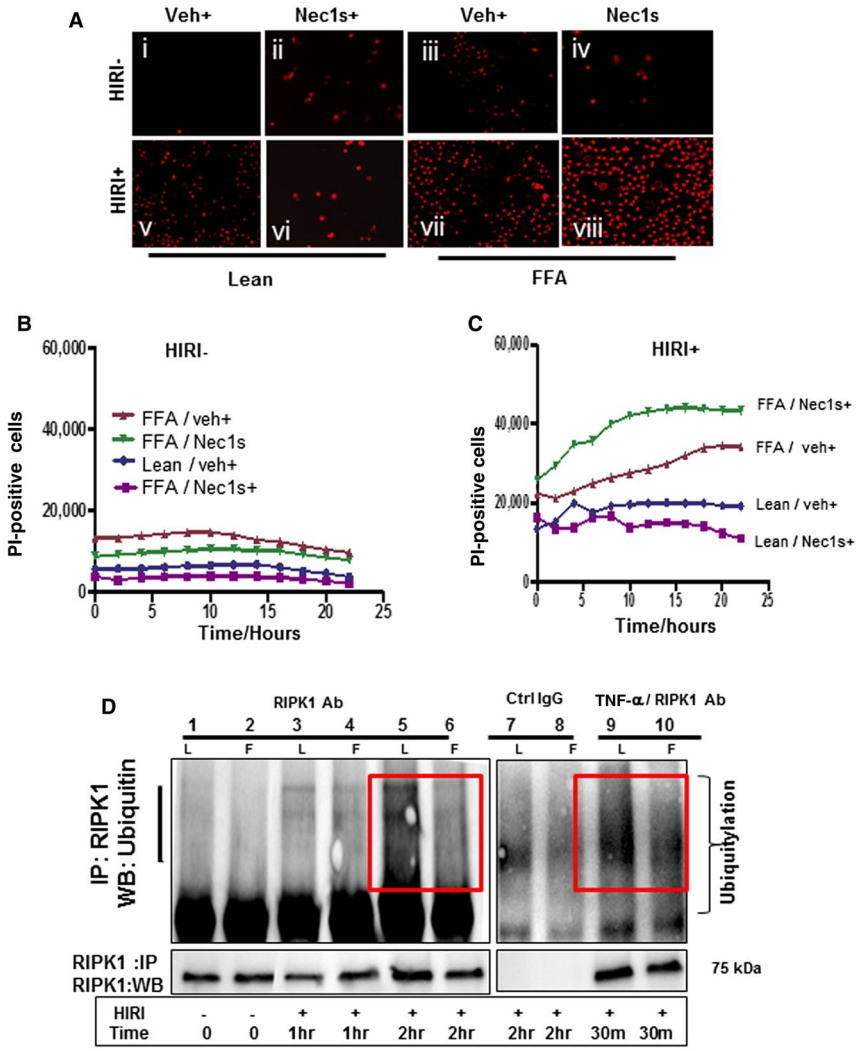

FIG. 4. Blockade of RIPK1 by Nec1s *in vitro* demonstrated increased cell death in FFA-treated AML12 cells. Lean and FFA-treated AML12 cells were treated with vehicle and Nec1s (30 μm) 30 minutes before HIRI. (A) Top panel shows lean controls of AML12 cells (A-i veh+, A-ii Nec1s+) and FFA controls (A-iii veh+, A-iv Nec1s+). Bottom panel shows lean (A-v veh+, A-vi Nec1s+) and FFA (A-vii veh+, A-viii Nec1s+) undergoing HIRI (scale is 20×). Red fluorescence represents number of PI-positive dead cells. As shown here, FFA HIRI Nec1s+ (A-viii) demonstrated a significant increase in PI-positive cells compared to FFA HIRI veh+ (A-vii). (B) Live imaging of the PI uptake is monitored by the Incucyte Zoom system in lean and FFA mice without HIRI. (C) FFA HIRI Nec1s+ demonstrated a significant increase in cell death (number of PI-positive cells; green line) compared to FFA veh+ (red line), whereas lean HIRI Nec1s+ (purple line) showed fewer PI-positive cells compared to lean HIRI veh+ (blue line). (D) Lean and FFA-treated AML12 cells were subjected to HIRI for 40 minutes followed by 30 minutes, 1 hour, and 2 hours of reperfusion. MG-132 (10 μM) was added to the media to prevent deubiquitylation. One milligram of total protein from cell lysate of lean HIRI and FFA HIRI were immunoprecipitated by RIPK1-specific antibody (5 μg/mL lysate) to pull down proteins bound to RIPK1; IgG was used as a negative control. These pellets were run on SDS-PAGE followed by western blotting with ubiquitin antibody. Lanes 1 and 2 were lean and FFA controls, lanes 3 and 4 were HIRI (1 hour), lanes 5 and 6 were HIRI 2 hours, lanes 7 and 8 were negative control (IgG), and lanes 9 and 10 were positive control (TNF-α (1 μg/mL). Positive ubiquitin band was seen in lean HIRI (lane 5) at 2 hours but not observed in the FFA HIRI (lane 6). Bottom panel shows RIPK1 bands of the same blot reprobed with RIPK1 antibody. Abbreviations: Ab, antibody; Ctrl, control; hr, hour; IP, immunoprecipitation; m, minute; veh, vehicle.

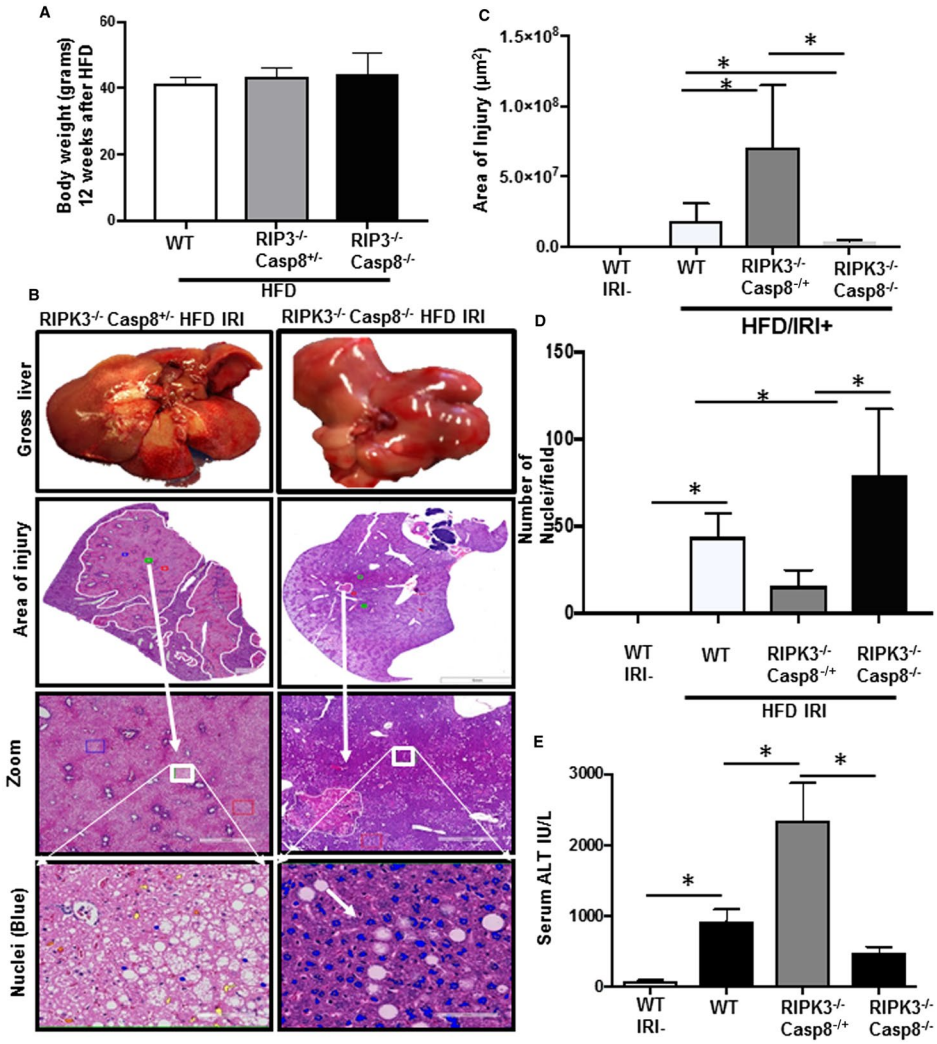

FIG. 5. Steatotic liver injury is not mediated through RIPK3 signaling but is mediated through Casp8 signaling. Rectangle represents the area that was zoomed in the panel below. (A) Body weights of WT and RIP3$^{-/-}$/Casp8$^{-/+}$ and RIP3$^{-/-}$/Casp8$^{-/-}$ mice demonstrated similar weight gain compared to WT mice fed an HFD. (B) Representative images of liver sections from HFD-fed mice 24 hours after IRI are depicted; RIP3$^{-/-}$/Casp8$^{-/+}$ (left panel) RIP3$^{-/-}$/Casp8$^{-/-}$ (right panel). Gross images (first row), H&E stained liver lobe showing the areas of injury marked by white lines (second row), zoomed images of the area of injury (third row, 4×), and intact nuclei (blue, fourth row, 40×) are depicted. (C) RIP3$^{-/-}$/Casp8$^{-/+}$ mice showed significant increase in area of injury (*P < 0.001). (D) Graph shows significantly low intact nuclei (blue; *P < 0.0001). (E) There was a significant reduction in serum ALT (*P < 0.002) compared to RIP3$^{-/-}$/Casp8$^{-/-}$ (n = 10). Data represent mean ± SD.

immunofluorescence with cleaved Casp8 antibody (Fig. 6B), staining was significantly higher in FFA-treated AML12 cells undergoing HIRI. Further, there was a significant increase in Casp8 mRNA at 6 hours after IRI in livers of HFD-fed mice (P < 0.0001; Fig. 6C), which was corroborated by a significant increase in Casp8 protein staining (Fig. 6D). In addition, western blot analysis of total liver protein lysates from HFD-fed mice after IRI showed increased cleaved Casp8 levels at 2 and 6 hours after IRI (Fig. 6E). A significant increase in Casp8 activity was observed in Nec1s-treated steatotic AML12 cells (P < 0.004; Fig. 6F), whereas Casp8 activity was significantly lowered with Nec1s treatment in lean cells (P < 0.03; Fig. 6F). In addition, human liver biopsy sections from subjects with NASH showed a significant increase in staining intensity of cleaved Casp8 (Fig. 7D,F) compared to lean human liver (Fig. 7C,F), confirming

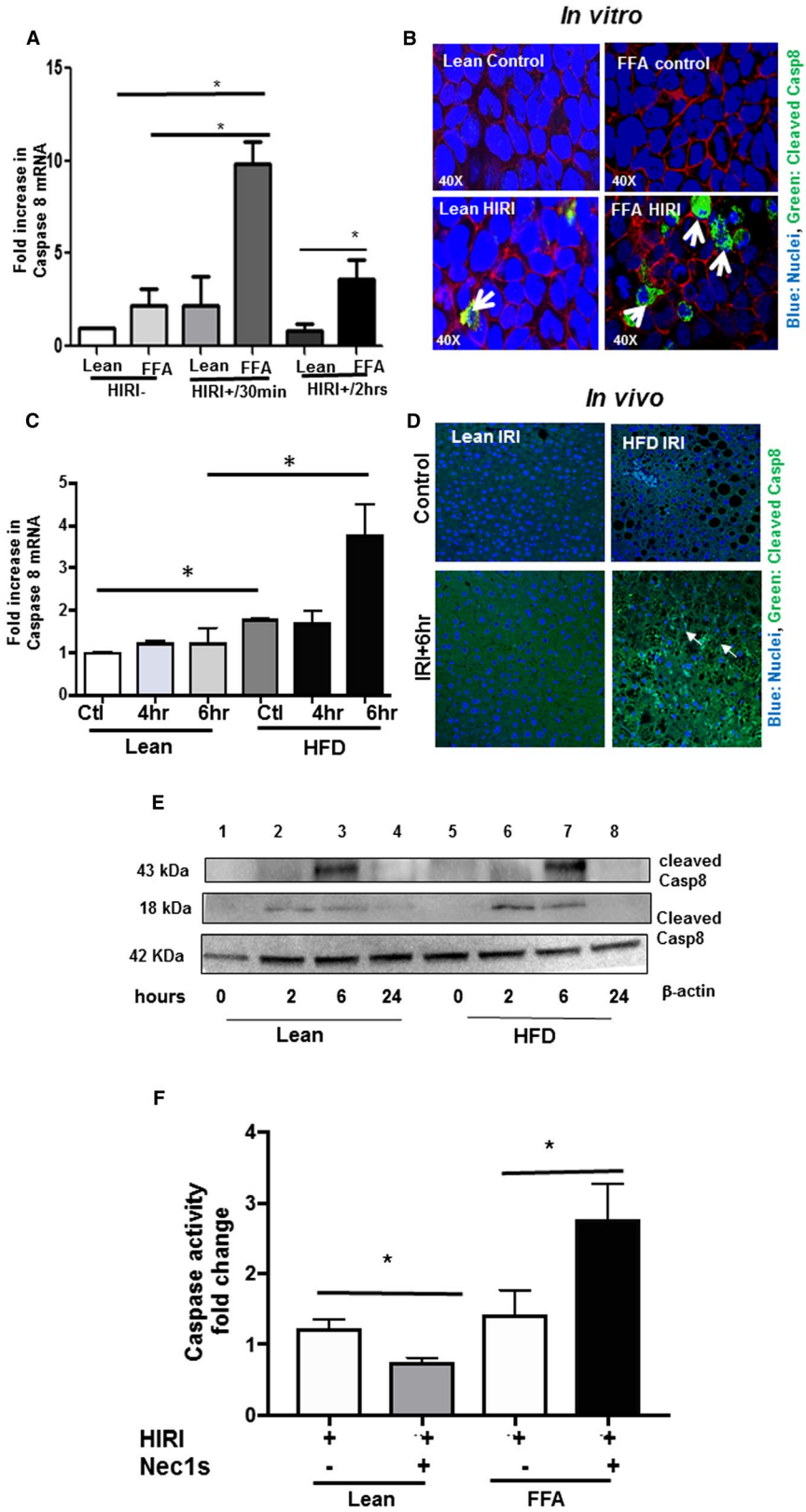
A
Fold increase in Caspase 8 mRNA
15
10
5
0
*
*
*
Lean
FFA
Lean
FFA
Lean
FFA
HIRI-
HIRI+/30min
HIRI+/2hrs
B
In vitro
Lean Control
FFA control
Lean HIRI
FFA HIRI
40X
Blue: Nuclei, Green: Cleaved Casp8
C
Fold increase in Caspase 8 mRNA
5
4
3
2
1
0
*
*
Ctl
4hr
6hr
Ctl
4hr
6hr
Lean
HFD
D
In vivo
Lean IRI
HFD IRI
Control
IRI+6hr
Blue: Nuclei, Green: Cleaved Casp8
E
1 2 3 4 5 6 7 8
43 kDa
cleaved Casp8
18 kDa
Cleaved Casp8
42 KDa
hours 0 2 6 24 0 2 6 24
β-actin
Lean
HFD
F
Caspase activity fold change
4
3
2
1
0
*
*
HIRI
Nec1s
+ + + +
- + - +
Lean
FFA

FIG. 6. RIPK1 blockade leads to increased Casp8 activity in HFD-fed mice liver and FFA-treated AML12 cells. Arrows represent Casp8 staining. (A) Fold change in mRNA levels of Casp8 in lean HIRI and FFA HIRI (30 minutes and 2 hours) compared to lean controls. FFA-treated HIRI cells showed significant increase in mRNA compared to lean HIRI at 30 minutes (*$P < 0.01$). (B) Both lean FFA-treated HIRI cells were fixed and subjected to immunofluorescence with cleaved Casp8 antibody (green), as described in Materials and Methods, counterstained by DAPI (blue, nuclei) membrane stain (red). (C) Fold change in Casp8 mRNA from lean and HFD IRI at various time intervals (0, 4, and 6 hours after IRI). Casp8 mRNA in HFD IRI (6 hours) showed significant increase compared to lean IRI (*$P < 0.0001$). (D) Liver tissues showing cleaved Casp8 (green) staining in lean and HFD IRI after 6 hours, counterstained with DAPI (blue, nuclei). (E) Total proteins from lean and HFD mice livers undergoing IRI for 2, 6, and 24 hours were subjected to SDS-PAGE and probed with cleaved Casp8 antibody, as described in Materials and Methods. Cleaved Casp8 43 kDa (top), 18 kDa (middle), loading control β-actin (bottom panel). Lanes 1-4 represent lean and lanes 5-8 depict HFD mice. (F) Total cell lysates from lean HIRI veh+, lean HIRI Nec1s+, FFA HIRI veh+, and FFA HIRI Nec1s+ were processed to measure Casp8 activity, using the Casp8 activity assay kit as described in Materials and Methods. FFA-treated HIRI Nec1s+ cells demonstrated significant increase in Casp8 activity compared to FFA HIRI veh+ (*$P < 0.004$). However, lean HIRI Nec1s+ showed decreased Casp8 activity compared to lean HIRI veh+ (*$P < 0.03$). Data represent mean ± SD. Abbreviations: Ctl, control; hr or hrs, hours; min, minutes; veh, vehicle.

the translational significance of Casp8-mediated cell death in human NASH.

RIPK1 BLOCKADE LEADS TO MITOCHONDRIAL DAMAGE IN HFD-FED MICE LIVERS THAT WAS REVERSED IN BID$^{-/-}$ MICE UNDERGOING IRI

To assess morphology of cell death at a cellular level, we performed electron microscopy of livers from HFD-fed mice undergoing IRI. Mitochondrial damage was seen with distorted membrane and cristae (Fig. 8A). Mitochondrial survival was also measured, and the percentage of live cells was significantly decreased ($P < 0.001$) in Nec1s-treated steatotic AML12 cells undergoing HIRI compared to lean cells with Nec1s undergoing HIRI. FFA-treated AML12 cells showed significantly reduced cell survival, which was further reduced significantly with Nec1s treatment (Fig. 8C). In addition, Nec1s-treated HFD-fed steatotic liver showed increased TUNEL-positive staining, suggesting increased apoptosis in steatotic liver undergoing IRI (Fig. 8D). It is known that cleavage of BID by Casp8 mediates mitochondrial damage[39]; we therefore subjected HFD-fed BID$^{-/-}$ mice to IRI. HFD-fed BID$^{-/-}$ mice showed significant protection, which was demonstrated by decreased injury score ($P < 0.03$) and lower serum ALT ($P < 0.004$; Fig. 8E,F). These results suggest that exacerbated hepatocellular injury in steatotic liver undergoing IRI is mediated by Casp8-dependent cell death through BID signaling. A schematic representation of RIPK1-mediated multimodal signaling events during steatotic liver undergoing IRI is shown in Fig. 9.

Discussion

Although increased susceptibility to injury of steatotic liver has been reported in the clinical literature, little is known about the underlying molecular mechanisms and pathways. Through the analysis of the extent of liver damage and hepatocyte cell death by RIPK1 blockade, we have serendipitously found that RIPK1 inhibition under steatotic liver conditions triggers exacerbation of hepatocellular death following IRI. This finding was completely unexpected and in contrast to the widely accepted concept that RIPK1 inhibition is protective, thereby reducing damage following ischemic injury in brain,[36] heart,[40] kidney,[41] and liver.[42,43] We also demonstrated that inhibition of RIPK3, a critical component of the necrosome, leads to hepatocellular death in steatotic liver while conferring protection in the lean liver, underscoring the fact that cell death in a steatotic liver is not mediated by RIP3 as occurs in the lean liver. Our data determined that ubiquitylation of RIPK1 was present in lean but decreased in steatotic liver/hepatocytes undergoing IRI. Importantly, we discovered that the mechanism of increased hepatocellular injury in steatotic liver following RIPK1 inhibition was mediated through the Casp8 pathway because loss of Casp8 signaling led to protection in the HFD-fed mice from IRI. This alludes to an apoptotic form of cell death, which was operational exclusively in the steatotic liver and not

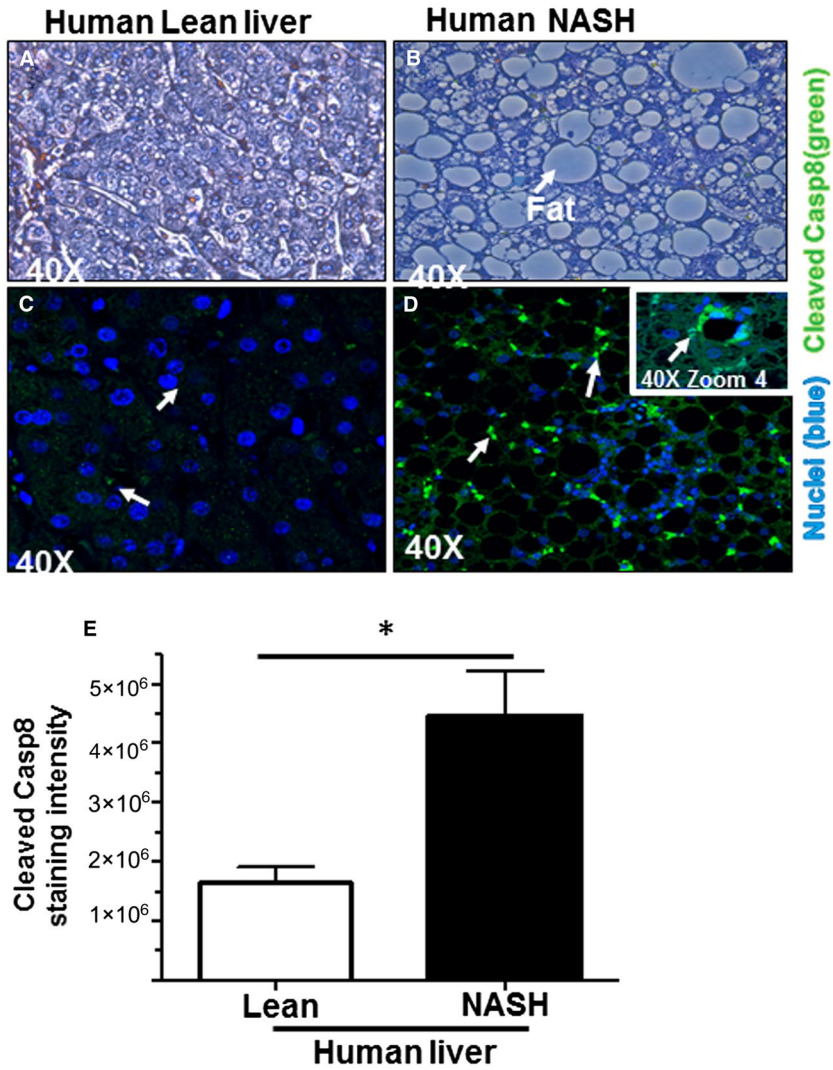

FIG. 7. Human NASH liver biopsy shows increased expression of cleaved Casp8. (A-D) Paraffin sections of human lean control (A,C) and NASH (B,D) sections were obtained as shown in the Materials and Methods. Top panel represents H&E, and bottom panel represents immunofluorescence with cleaved Casp8 antibody (green) counterstained by nuclear stain (blue, DAPI) as described in Materials and Methods. (E) Quantification of Casp8 staining intensity by Fiji ImageJ software showed significant increase in cleaved Casp8 staining in NASH samples compared to lean controls (*$P < 0.003$; n = 6). Data represent mean ± SD.

in the lean liver. The canonical outcome of RIPK1 inhibition has been Casp8 inhibition, and our study reveals a previously unknown effect of RIPK1 inhibition leading to increased Casp8-mediated cell death, which is operational only in the presence of steatosis within the same cell. With human NAFLD data also confirming increased expression of Casp8 in the steatotic liver, this becomes a crucial area of investigation, and studies are in progress to further delineate the mechanism of RIPK1 blockade in activating Casp8.

RIP1 and RIP3 kinases are thought to play a principal role in the execution of necroptosis,[44] and blocking their kinase functions has been shown to confer protection from TNF-α-induced necroptotic death following IRI of various organs.[36,40,41] Being a key component of the TNFR1 signaling complex, however, RIPK1 signaling triggers a wide variety of physiologic responses ranging from TNF-α-dependent cell survival and proliferation[27,45] to apoptotic and necroptotic death,[46,47] thus mimicking the complexity of cellular responses to TNF-α.

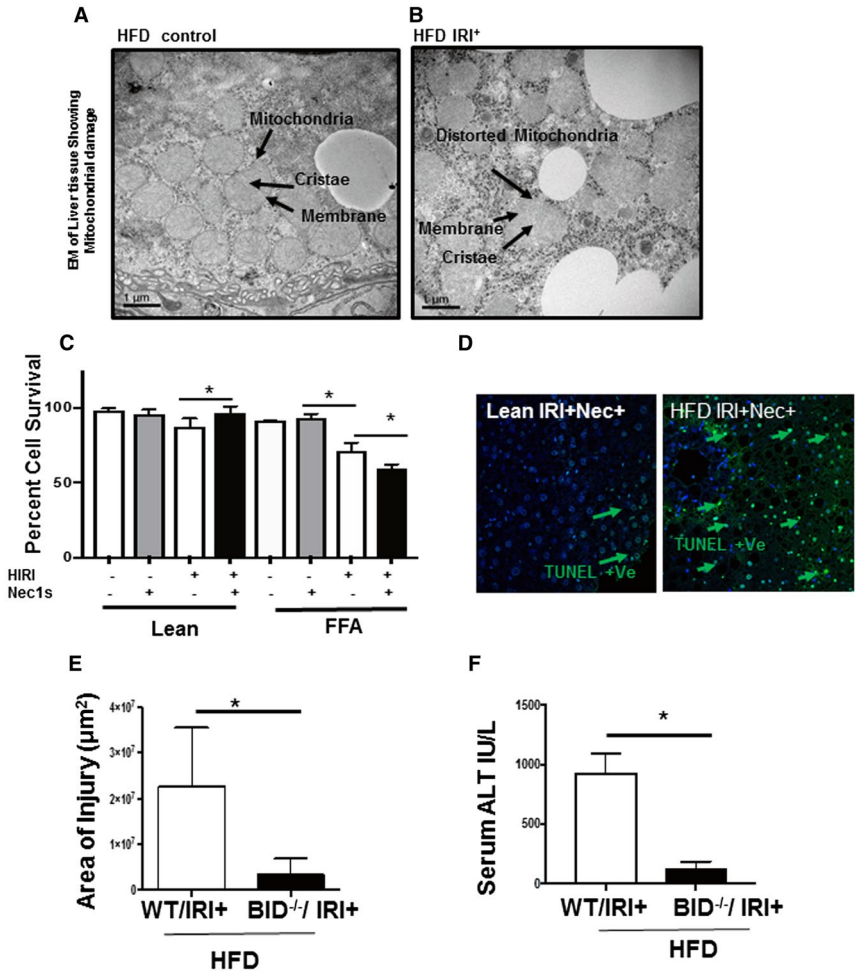

FIG. 8. RIPK1 blockade leads to mitochondrial damage in HFD-fed mice livers that was reversed in $BID^{-/-}$ mice undergoing IRI. (A) Representative electron micrograph of HFD control mouse liver shows intact mitochondria. (B) EM of HFD IRI shows distorted mitochondria (broken membrane and cristae), represented by the arrow. (C) Mitochondrial viability assessed by the MTT assay, as described in Materials and Methods. FFA-treated HIRI Nec1s+ demonstrated significantly low percent viability compared to FFA-treated HIRI veh+ (*$P < 0.001$). In contrast, lean HIRI Nec1s+ cells showed increased viability compared to lean HIRI veh+ (*$P < 0.001$). (D) Liver tissues from lean IRI Nec1s+ (left panel) and HFD IRI Nec1s+ (right panel) were processed for TUNEL staining, as described in Materials and Methods. TUNEL-positive cells representing apoptotic cells were stained green and were higher in HFD IRI Nec1s+ compared to lean IRI Nec1s+. (E) Area of injury in WT HFD IRI versus $BID^{-/-}$ HFD IRI. As shown here $BID^{-/-}$ mice showed a significant reduction in injury area (*$P < 0.03$). (F) Serum ALT levels were significantly lower than WT HFD IRI (*$P < 0.004$; n = 10). Data represent mean ± SD. Abbreviations: +Ve, positive; EM, electron microscopy; MTT, 3-(4,5-dimethylthiazol-2-yl)-2,5-diphenyltetrazolium bromide; veh, vehicle.

Although RIPK1 and RIPK3 are both functionally active phosphokinases, their substrate specificity remains unknown. Our data showed that blocking kinase activity of RIPK1 leads to a significant exacerbation of liver injury in response to ischemia–reperfusion in a steatotic liver environment. This is in stark contrast to other reports that have shown a protective role of RIPK1 inhibition in IRI, making this an important finding when considering RIPK1 inhibition in the clinical setting.

RIPK1 is highly regulated, most notably by phosphorylation and ubiquitylation.[38] Following TNFR1 stimulation, and depending on intracellular contexts, RIPK1 is ubiquitylated by K63 or linear chain ubiquitination, and these events trigger the recruitment of downstream signaling kinases (most critically the

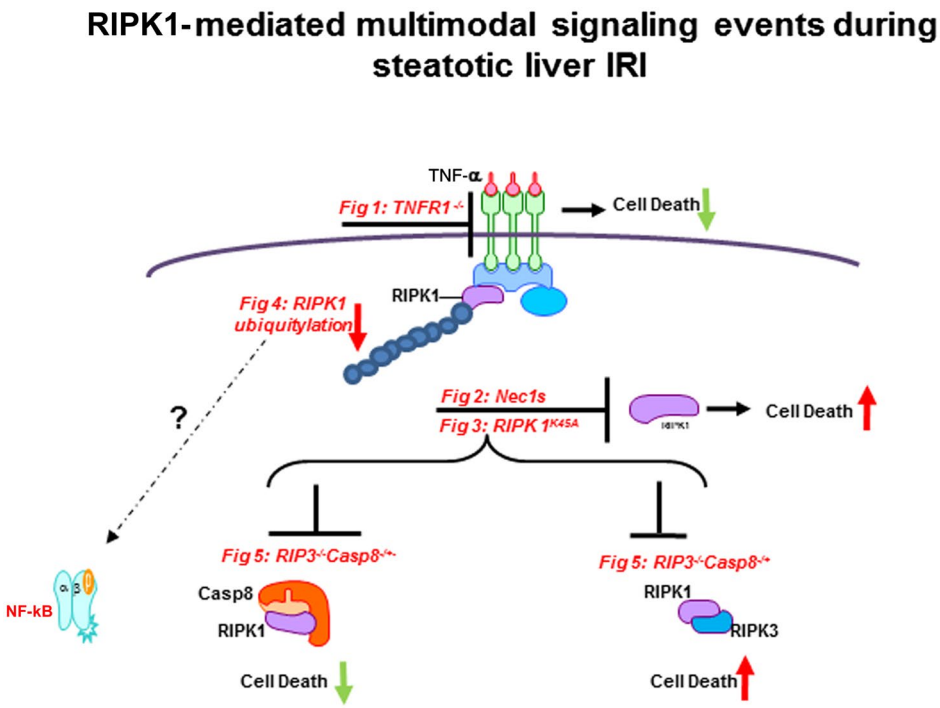

FIG. 9. Schematic representation of RIPK1-mediated multimodal signaling events during steatotic liver undergoing IRI.

linear ubiquitin chain assembly complex [LUBAC]) that activate several signal transduction pathways, ultimately leading to activation of nuclear factor kappa B (NF-κB), leading to cell survival. Although the precise ligase site and form remains to be dissected in greater depth, we found that ubiquitination of RIPK1 was present in lean liver/hepatocytes and decreased in steatotic liver/hepatocytes at baseline and after IRI. These data suggest that RIPK1 ubiquitylation might be a critical switch point in determining the fate of steatotic versus lean liver/hepatocyte when exposed to secondary injury. RIPK1 ubiquitylation has been shown to be altered under stress environments, which can lead to Fas-associated protein with death domain (FADD) initiating Casp8-dependent apoptosis.[48-50] Unexpectedly, our data showed that RIPK1 inhibition leads to increased Casp8 activity in the steatotic liver that was also increased at baseline but further amplified with RIPK1 inhibition. HFD-fed RIP3$^{-/-}$/Casp8$^{-/-}$ mice showed protection from IRI, confirming the presence of apoptotic cell death as this protection was not seen in HFD-fed RIP3$^{-/-}$/Casp8$^{-/+}$ mice, affirming that cell death was not RIP3 mediated. However, several reports support that RIP1 kinase activity is required for Casp8-mediated cell death, but some oppose this notion in certain cell types. Our data show that Casp8 activity is up-regulated with increased cell death phenotype in the absence of RIP1 kinase activity. To our knowledge, this is the first report of Casp8-mediated cell death in the steatotic liver that is activated by inhibition of RIP1 kinase activity exclusively in the presence of steatosis, indicating that RIP1 kinase activity is essential in a steatotic environment. Whether this caspase-mediated effect in the absence of RIPK1 is modulated by adaptation of multiple signaling proteins, such as NF-κB, cellular FLICE-like inhibitory proteins (cFLIP), or cellular inhibitor of apoptosis proteins (cIAPs), or is a process directly linked to RIPK1 ubiquitylation or scaffolding function is currently under investigation.

This study proposes that RIPK1 inhibition leads to Casp8-mediated exacerbated cell death in the steatotic liver whereas it protects the lean liver from cell death and for the first time demonstrates the RIPK1 signaling switches within the same cell type (hepatocyte) based on the intracellular environment, i.e., the presence of steatosis. Human steatotic liver also shows increased expression of Casp8, thus confirming the

translational significance of this finding and opening a critical area of investigation for future studies in steatotic liver injury in patients with NAFLD.

Acknowledgment: We are thankful to V. Dixit and Kim Newton (Roche, CA) for RIPK3$^{-/-}$ mice, R. Hakem (University of Toronto) for mice with Casp8$^{fl/fl}$ allele, RIPK1^{-K45A} mice were provided by Dr. John Bertin (Glaxo-Smith-Klein), BID$^{-/-}$ mice were kindly provided by A. Strasser (The Walter and Eliza Hall Institute of Medical Research, Australia). We acknowledge Emory Animal Physiology core, ICI core, CHOA and Winship Pathology core for their support.

REFERENCES

1) Younossi Z, Anstee QM, Marietti M, Hardy T, Henry L, Eslam M, et al. Global burden of NAFLD and NASH: trends, predictions, risk factors and prevention. Nat Rev Gastroenterol Hepatol 2018;15:11-20.
2) Mahady SE, George J. Management of nonalcoholic steatohepatitis: an evidence-based approach. Clin Liver Dis 2012; 16:631-645.
3) Baffy G. Hepatocellular carcinoma in non-alcoholic fatty liver disease: epidemiology, pathogenesis, and prevention. J Clin Transl Hepatol 2013;1:131-137.
4) Wree A, Broderick L, Canbay A, Hoffman HM, Feldstein AE. From NAFLD to NASH to cirrhosis-new insights into disease mechanisms. Nat Rev Gastroenterol Hepatol 2013;10: 627-636.
5) Vucur M, Reisinger F, Gautheron J, Janssen J, Roderburg C, Cardenas DV, et al. RIP3 inhibits inflammatory hepatocarcinogenesis but promotes cholestasis by controlling caspase-8- and JNK-dependent compensatory cell proliferation. Cell Rep 2013;4:776-790.
6) Chavin KD, Fiorini RN, Shafizadeh S, Cheng G, Wan C, Evans Z, et al. Fatty acid synthase blockade protects steatotic livers from warm ischemia reperfusion injury and transplantation. Am J Transplant 2004;4:1440-1447.
7) Clavien PA, Selzner M. Hepatic steatosis and transplantation. Liver Transpl 2002;8:980.
8) Jaeschke H. Role of reactive oxygen species in hepatic ischemia-reperfusion injury and preconditioning. J Invest Surg 2003;16:127-140.
9) Gujral JS, Bucci TJ, Farhood A, Jaeschke H. Mechanism of cell death during warm hepatic ischemia-reperfusion in rats: apoptosis or necrosis? Hepatology 2001;33:397-405.
10) Gupta NA, Kolachala VL, Jiang R, Abramowsky C, Romero R, Fifadara N, et al. The glucagon-like peptide-1 receptor agonist Exendin 4 has a protective role in ischemic injury of lean and steatotic liver by inhibiting cell death and stimulating lipolysis. Am J Pathol 2012;181:1693-1701.
11) **Gupta NA**, **Kolachala VL**, Jiang R, Abramowsky C, Shenoi A, Kosters A, et al. Mitigation of autophagy ameliorates hepatocellular damage following ischemia reperfusion injury in murine steatotic liver. Am J Physiol Gastrointest Liver Physiol 2014;307:G1088-G1099.
12) Kolachala VL, Palle S, Shen M, Feng A, Shayakhmetov D, Gupta NA. Loss of L-selectin-guided CD8(+), but not CD4(+), cells protects against ischemia reperfusion injury in a steatotic liver. Hepatology 2017;66:1258-1274.
13) Weng J, Li W, Jia X, An W. Alleviation of ischemia-reperfusion injury in liver steatosis by augmenter of liver regeneration is attributed to antioxidation and preservation of mitochondria. Transplantation 2017;101:2340-2348.
14) Dela Pena A, Leclercq I, Field J, George J, Jones B, Farrell G. NF-kappaB activation, rather than TNF, mediates hepatic inflammation in a murine dietary model of steatohepatitis. Gastroenterology 2005;129:1663-1674.
15) Wegner KW, Saleh D, Degterev A. Complex pathologic roles of RIPK1 and RIPK3: moving beyond necroptosis. Trends Pharmacol Sci 2017;38:202-225.
16) Newton K. RIPK1 and RIPK3: critical regulators of inflammation and cell death. Trends Cell Biol 2015;25:347-353.
17) Galluzzi L, Aaronson SA, Abrams J, Alnemri ES, Andrews DW, Baehrecke EH, et al. Guidelines for the use and interpretation of assays for monitoring cell death in higher eukaryotes. Cell Death Differ 2009;16:1093-1107.
18) Linkermann A, Green DR. Necroptosis. N Engl J Med 2014;370:455-465.
19) Kanneganti TD, Ozoren N, Body-Malapel M, Amer A, Park JH, Franchi L, et al. Bacterial RNA and small antiviral compounds activate caspase-1 through cryopyrin/Nalp3. Nature 2006;440:233-236.
20) Martinon F, Tschopp J. Inflammatory caspases and inflammasomes: master switches of inflammation. Cell Death Differ 2007;14:10-22.
21) Kim YM, Kim TH, Chung HT, Talanian RV, Yin XM, Billiar TR. Nitric oxide prevents tumor necrosis factor alpha-induced rat hepatocyte apoptosis by the interruption of mitochondrial apoptotic signaling through S-nitrosylation of caspase-8. Hepatology 2000;32:770-778.
22) Feldstein AE, Canbay A, Angulo P, Taniai M, Burgart LJ, Lindor KD, et al. Hepatocyte apoptosis and fas expression are prominent features of human nonalcoholic steatohepatitis. Gastroenterology 2003;125:437-443.
23) Freimuth J, Bangen JM, Lambertz D, Hu W, Nevzorova YA, Sonntag R, et al. Loss of caspase-8 in hepatocytes accelerates the onset of liver regeneration in mice through premature nuclear factor kappa B activation. Hepatology 2013;58:1779-1789.
24) Zhang DW, Shao J, Lin J, Zhang N, Lu BJ, Lin SC, et al. RIP3, an energy metabolism regulator that switches TNF-induced cell death from apoptosis to necrosis. Science 2009;325:332-336.
25) Vandenabeele P, Galluzzi L, Vanden Berghe T, Kroemer G. Molecular mechanisms of necroptosis: an ordered cellular explosion. Nat Rev Mol Cell Biol 2010;11:700-714.
26) Cho YS, Challa S, Moquin D, Genga R, Ray TD, Guildford M, et al. Phosphorylation-driven assembly of the RIP1-RIP3 complex regulates programmed necrosis and virus-induced inflammation. Cell 2009;137:1112-1123.
27) Takahashi N, Vereecke L, Bertrand MJ, Duprez L, Berger SB, Divert T, et al. RIPK1 ensures intestinal homeostasis by protecting the epithelium against apoptosis. Nature 2014;513:95-99.
28) Dannappel M, Vlantis K, Kumari S, Polykratis A, Kim C, Wachsmuth L, et al. RIPK1 maintains epithelial homeostasis by inhibiting apoptosis and necroptosis. Nature 2014;513:90-94.
29) Silke J, Rickard JA, Gerlic M. The diverse role of RIP kinases in necroptosis and inflammation. Nat Immunol 2015;16: 689-697.
30) Mandal P, Feng Y, Lyons JD, Berger SB, Otani S, DeLaney A, et al. Caspase-8 collaborates with caspase-11 to drive tissue damage and execution of endotoxic shock. Immunity 2018;49:42-55.e46.
31) Berger SB, Kasparcova V, Hoffman S, Swift B, Dare L, Schaeffer M, et al. Cutting edge: RIP1 kinase activity is dispensable for normal development but is a key regulator of inflammation in SHARPIN-deficient mice. J Immunol 2014;192:5476-5480.

32) Kaiser WJ, Upton JW, Long AB, Livingston-Rosanoff D, Daley-Bauer LP, Hakem R, et al. RIP3 mediates the embryonic lethality of caspase-8-deficient mice. Nature 2011;471:368-372.
33) Degterev A, Maki JL, Yuan J. Activity and specificity of necrostatin-1, small-molecule inhibitor of RIP1 kinase. Cell Death Differ 2013;20:366.
34) Takemoto K, Hatano E, Iwaisako K, Takeiri M, Noma N, Ohmae S, et al. Necrostatin-1 protects against reactive oxygen species (ROS)-induced hepatotoxicity in acetaminophen-induced acute liver failure. FEBS Open Bio 2014;4:777-787.
35) Thackaberry EA, Wang X, Schweiger M, Messick K, Valle N, Dean B, et al. Solvent-based formulations for intravenous mouse pharmacokinetic studies: tolerability and recommended solvent dose limits. Xenobiotica 2014;44:235-241.
36) Fricker M, Vilalta A, Tolkovsky AM, Brown GC. Caspase inhibitors protect neurons by enabling selective necroptosis of inflamed microglia. J Biol Chem 2013;288:9145-9152.
37) Udeshi ND, Mani DR, Eisenhaure T, Mertins P, Jaffe JD, Clauser KR, et al. Methods for quantification of in vivo changes in protein ubiquitination following proteasome and deubiquitinase inhibition. Mol Cell Proteomics 2012;11:148-159.
38) Peltzer N, Darding M, Walczak H. Holding RIPK1 on the ubiquitin leash in TNFR1 signaling. Trends Cell Biol 2016;26:445-461.
39) DuBray BJ Jr., Conzen KD, Upadhya GA, Gunter KL, Jia J, Knolhoff BL, et al. BH3-only proteins contribute to steatotic liver ischemia-reperfusion injury. J Surg Res 2015;194:653-658.
40) Luedde M, Lutz M, Carter N, Sosna J, Jacoby C, Vucur M, et al. RIP3, a kinase promoting necroptotic cell death, mediates adverse remodelling after myocardial infarction. Cardiovasc Res 2014;103:206-216.
41) Lau A, Wang S, Jiang J, Haig A, Pavlosky A, Linkermann A, et al. RIPK3-mediated necroptosis promotes donor kidney inflammatory injury and reduces allograft survival. Am J Transplant 2013;13:2805-2818.
42) Roychowdhury S, McMullen MR, Pisano SG, Liu X, Nagy LE. Absence of receptor interacting protein kinase 3 prevents ethanol-induced liver injury. Hepatology 2013;57:1773-1783.
43) Deutsch M, Graffeo CS, Rokosh R, Pansari M, Ochi A, Levie EM, et al. Divergent effects of RIP1 or RIP3 blockade in murine models of acute liver injury. Cell Death Dis 2015;6:e1759.
44) Zhang D, Lin J, Han J. Receptor-interacting protein (RIP) kinase family. Cell Mol Immunol 2010;7:243-249.
45) Festjens N, Vanden Berghe T, Cornelis S, Vandenabeele P. RIP1, a kinase on the crossroads of a cell's decision to live or die. Cell Death Differ 2007;14:400-410.
46) Tomita K, Tamiya G, Ando S, Ohsumi K, Chiyo T, Mizutani A, et al. Tumour necrosis factor alpha signalling through activation of Kupffer cells plays an essential role in liver fibrosis of non-alcoholic steatohepatitis in mice. Gut 2006;55:415-424.
47) Hitomi J, Christofferson DE, Ng A, Yao J, Degterev A, Xavier RJ, et al. Identification of a molecular signaling network that regulates a cellular necrotic cell death pathway. Cell 2008;135:1311-1323.
48) Feoktistova M, Geserick P, Kellert B, Dimitrova DP, Langlais C, Hupe M, et al. cIAPs block Ripoptosome formation, a RIP1/caspase-8 containing intracellular cell death complex differentially regulated by cFLIP isoforms. Mol Cell 2011;43:449-463.
49) Tenev T, Bianchi K, Darding M, Broemer M, Langlais C, Wallberg F, et al. The Ripoptosome, a signaling platform that assembles in response to genotoxic stress and loss of IAPs. Mol Cell 2011;43:432-448.
50) Tait SW, Green DR. Mitochondria and cell death: outer membrane permeabilization and beyond. Nat Rev Mol Cell Biol 2010;11:621-632.

Author names in bold designate shared co-first authorship.

Supporting Information

Additional Supporting Information may be found at onlinelibrary.wiley.com/doi/10.1002/hep4.1352/suppinfo.